EFFECTS OF YARN PATH AND SUB-UNIT CELLS ON THE CHARACTERIZATION OF MECHANICAL PROPERTIES OF 3D BRAIDED COMPOSITE MATERIALS

Daniel R. Aldrich[1], and Cagri Ayranci[1*]

[1] Mechanical Engineering, University of Alberta
[*] Corresponding author: cayranci@ualberta.ca

Keywords: Braiding, FEM, Modelling, Textile Composites

ABSTRACT

Three-dimensional (3D) braided composite materials can provide improved in-plane and through thickness properties, while solving disadvantages faced by conventional composite materials. However, predicting their elastic and mechanical properties and behaviour can be difficult due to the additional undulations in the in-plane and out-of-plane directions compared to conventional laminated composites. Previous models that have been developed assume that the yarns travel along straight paths. This utilization of simplified geometry is an over simplification that is unable to account for the undulations in the 3D braided structure. These undulations in the fibres can lower the Young's modulus of the structure making the previous models inaccurate. A new method and model for the analysis of three-dimensional braids was developed to account for the undulations in the geometry. This model utilizes a sub-unit cell geometry that can be patterned to form the cross-section of the braided structure. The sub-unit cells consist of three types, namely: corner, edges, and centres. The sub-unit cell model was found to have varying results between the different types of sub-unit cells. These results can be attributed to the number of surface yarns within the sub-unit cell.

1 INTRODUCTION

Composite materials are becoming increasingly in demand due to the recent advancements and demands in the aviation, transportation, structural, and military applications [1]. These applications require materials with high specific stiffness and specific strength values, *i.e.*, stiffness and strength to weight ratios [1]. Conventional composite materials possess numerous benefits; however, they also suffer from drawbacks such as their low through-thickness properties and damage tolerances.

Braiding is an old textile composite manufacturing technique that has been adapted for use in advanced composite materials. Common applications include sports gear, medical devices, aviation industry as well as military applications. Traditionally, braided composite materials are divided into two main categories; namely two-dimensional (2D), and three-dimensional (3D) braiding [2, 3]. 3D braiding has the advantage over 2D braiding by providing additional interlocking of the yarns during the manufacturing process, see Figure 1, and form a solid structure. This in/out-of-plane interlocking of yarns increases the structural integrity of the 3D braided structure, preventing where some composites fail by delamination. However, these additional undulations cause complications when trying to predict the material properties and physical properties for design purposes. Because of the complications there is a need to develop geometric and finite element (FE) models to assist in predicting the behaviors and properties of these composite structures.

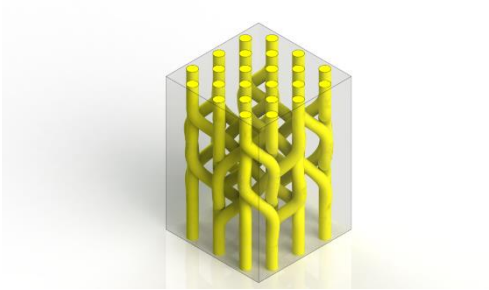

Figure 1: 3D braid architecture showing the interlocking of yarns created by emulation of the machine's fabrication method.

In literature, many analytical or finite element based models have been developed to predict or better understand the geometry of 3D braided structures [3, 4, 5, 6, 7, 8]. Most models are unable to represent the true geometric shape of the 3D braided structures, because the geometry is simplified or assumed, and not a function of the machine's movement. Often the models utilize "unit cells" that consist of yarn that travel along straight paths [3, 4, 5, 6]. This oversimplification of the undulating regions, rather than accounting for the actual path traveled by the yarn can lead to inaccurate results when determining the material properties.

This work concentrates on developing a geometric and set of FE models for a Cartesian rotary 3D braided composite material utilizing commercially available software. The model takes into account the machine's movements as well as the undulations within the braided structure to more accurately predict the Young's modulus. In this manuscript, the method to create the models is discussed. Additionally, the models are compared against existing models and are examined to determine the longitudinal Young's modulus.

2 METHODS

The path of the yarns, for the geometric model, is created in Matlab® by using the movements of the machine. The yarn paths are then passed to SolidWorks® where the geometric model of the yarns is created and assembled to form the model of the braided structure. Finally, the geometric model is transferred into Abaqus®, where the model is strained and the midplane normal force is determine and used to calculate the Young's modulus. The following sub-sections detail this methodology.

2.1 Development of the Geometric Paths

The geometric model is created by custom scripts written in two computer programs; the positioning and path of the yarns of the 3D braiding machine were generated using a commercial multi-paradigm numerical computing environment (Matlab® [9]), while the geometric model of the formed preform was created in a commercial solid modelling computer-aided design (CAD) program (SolidWorks® [10]). The custom scripts are accessible in their respective programs; however, they are also accessible through a custom graphical user interface (GUI), shown in Figure 2, designed to facilitate the design of the 3D braided structure with specific material properties. Properties of a braid can be estimated by the program, in the GUI, by having the theoretical limits for the material properties calculated, as well as by determining the Young's modulus with Professor Frank Ko's "Fabric Geometry Model" [4].

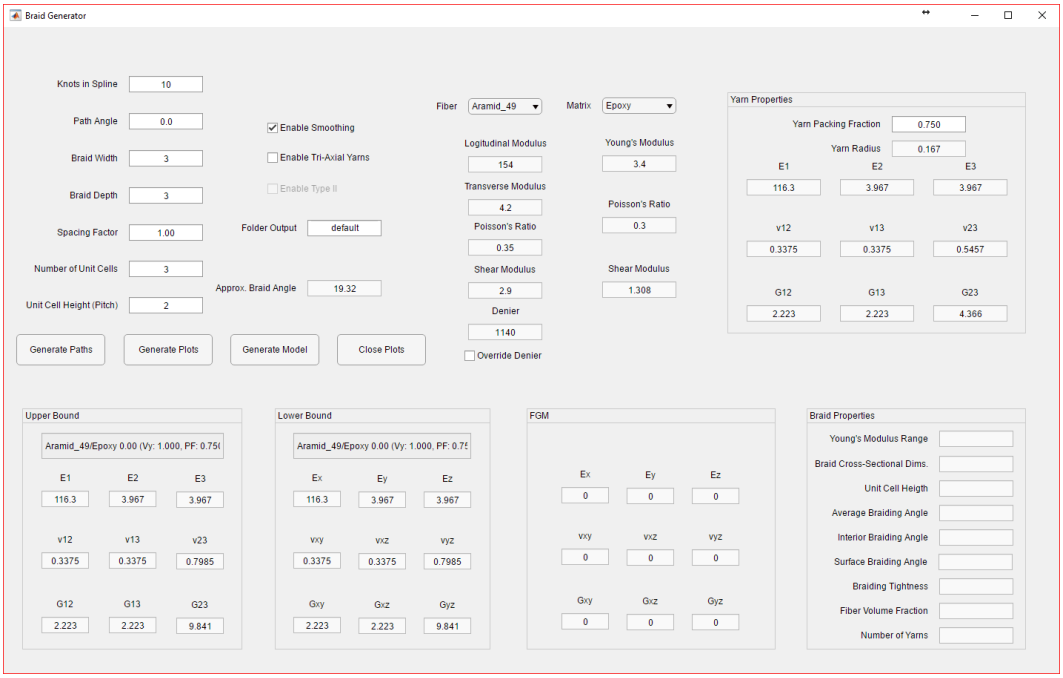

Figure 2: Graphical user interface, for the custom braiding program.

The first part of the program is used to create the braiding pattern; the braiding pattern is a collection of the final relative yarn positions at each step of braiding process. The positions of the yarns are found using a process regarded as machine emulation, whereby the stepwise positions of the yarn carriers are determined and used to find the position of the yarns [5]. For this study, a rotary braiding setup was chosen with a 2-step braiding pattern. This involves rotating the braiding cams in a checkerboard pattern with the even positions rotating in one direction during odd steps, and the odd positions rotating in the opposite direction during the even steps (Figure 3). The analysis used for this manuscript was done for a 3 x 3 cam set-up.

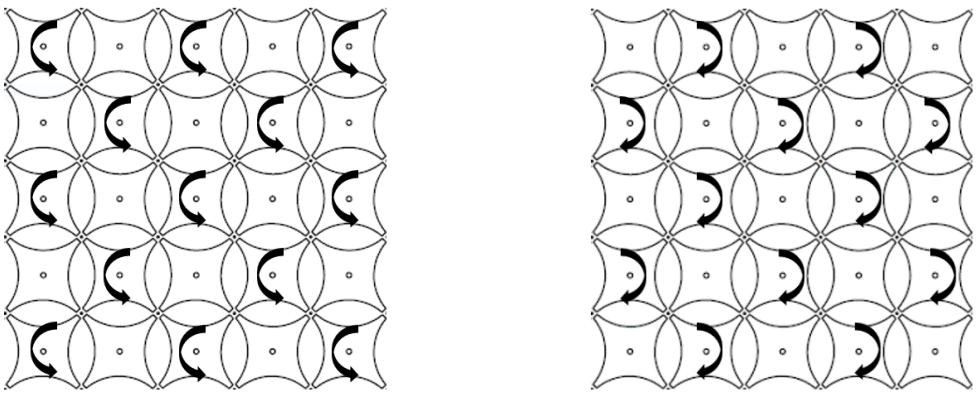

(a) (b)

Figure 3: 3D braiding process displaying the odd steps (a) and the even steps (b).

Next, the paths of the yarns are calculated to determine the yarn positions between the individual braiding steps. This is calculated assuming that the yarns travel straight paths between braiding steps, and that the distribution of points is evenly spaced based on the rotation of the cam. The relative yarn positions, *n* and *m*, are then converted to their actual positions, *y* and *z*, using a spacing factor and by taking in account the diameter of a yarn, shown by Equation (1).

$$\begin{bmatrix} y_i \\ z_i \end{bmatrix} = 2\ r\ SF \times \begin{bmatrix} n_i \\ m_i \end{bmatrix} \tag{1}$$

Where, r is the radius of a yarn, SF is the spacing factor, and i is the yarn number.

The physical path of a yarn is continuous and to help with the generation of the 3D geometry the paths are smoothed. The smoothing is accomplished by using an equal weighted convolution filter on each of the transverse (y-z) components. The filter is applied forwards and backwards to eliminate phase shifting effects in the axial direction [11]. As shown in Figure 4, the smoothed paths help eliminate sharp corners (discontinuities) in the path of the yarns that would cause problems in the generation of the 3D model, including self-intersecting geometry caused by the sudden change in direction. Additionally, the smoothing allows the yarns to be closer packed before the geometry starts to intersect with the other yarns, increasing the fiber volume fraction achievable with the model.

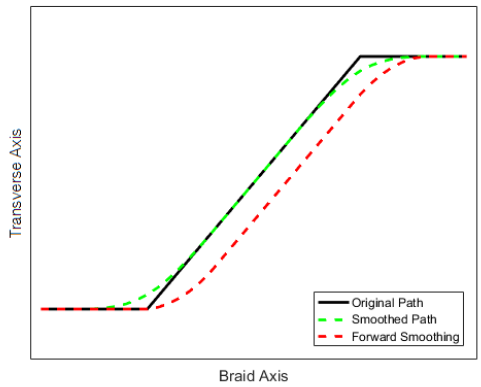

Figure 4: Example of the effect of smoothing on the path of a yarn in a single direction.

To generate the 3D model of the braid, the path of the yarns need to be passed from the one program to another. This is done by creating data files that contain the yarn paths in a CSV format and labeled appropriately, as to be read in by the next program. Additional data is written to another file, to aid in the creation of the CAD model; this file includes the general information about the braid, such as the yarn radius, number of active cams in the width and depth, the spacing factor, number of yarns, and the length of the braid. The second program is invoked by the first, by passing commands to the system to be executed in the command line. This opens the second program and once open the second program initiates a script that begins creating the 3D model, described later in section 2.2., *Development of the Geometric Model*.

The average angle of the yarns in the 3D braided structure and average yarn volume fraction are calculated geometrically from the paths that were generated; these values are used to determine a suitable range of values for the material properties based on unidirectional lamina. By selecting the materials for the fiber and the matrix, as well as the yarn packing fraction, the material properties of the yarn can be determined; finally, the properties of a unidirectional lamina can be calculated at a zero-degree angle and at the average angle of the 3D braided structure with the fiber volume fraction set to be the average yarn volume fraction calculated previously. The properties of these two unidirectional lamina act as the bounds for the properties of the 3D braid; due to the undulations in the 3D braided structure the modulus is expected to be lower than that of the zero-degree unidirectional lamina, thus forming the upper bound for the modulus. Additionally, because the interlocking yarns there is a higher degree of interaction in the in-plane and out-of-plane directions that results in the 3D

braided structure having a larger Young's modulus than that of a unidirectional angle lamina with an angle equal to the average yarn angle of the 3D braid.

2.2 Development of the Geometric Model

By utilizing the data files that were created previously, the 3D model of the braid can be created. The 3D model is created by a second program that was written in Visual Basic for Applications (VBA) that utilizes the SolidWorks API to automatically generate the assembly. The program first reads in the data file to determine the properties of the braid that are necessary to generate the geometry. After reading in the general data, the program steps through each of the individual yarn files and imports the data and converts the discrete points into a spline curve (Figure 5a). For each of the curves, the yarn cross-section is drawn on the top plane and centered on its respective curve end. The yarn is created by sweeping the cross-section along the curve that generates the solid geometry for the yarns. All the yarns are created in a single multibody part (Figure 5b). To complete the solid model of the yarns, the material properties are set to the part and the model is saved.

Next another part is created to represent the matrix of the braided structure. By using the number of active cams in the width and the depth, as well as the spacing factor, radius of the yarns, and the length of the braid, a solid block is created (Figure 5c). Like the yarns the material properties are set to the matrix and the model is also saved. Finally, an assembly is created by importing the two parts created previously aligning their origins and principle planes such that the two parts overlap each other. Next the matrix is edited in the assembly; cavities are created in the matrix by subtracting the yarns from the matrix. The feature is propagated back to the part and both the files are saved.

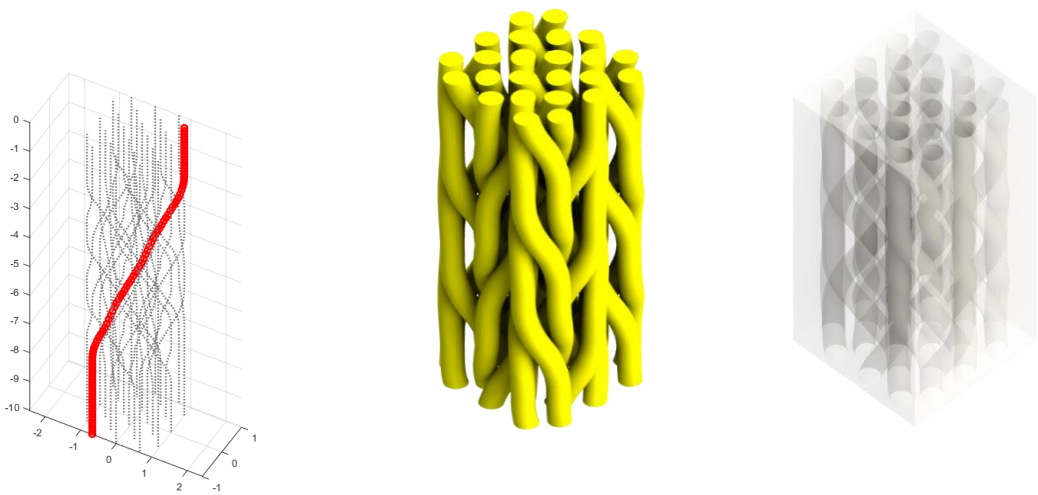

(a) (b) (c)

Figure 5: The paths (a), yarns (b), and the resin (c) that are used to create the completed geometric model of the 3D braided structure.

2.3 Development of the Finite Element Model

It is important to develop an FE model that can be analyzed in an efficient manor while accurately determining the properties of three-dimensionally braid composite material. The 3D model, created previously, is prepared for the FE analysis by first slicing the model into the appropriate unit cell geometry, and then the model is imported into the FEA software. For this study, the model was sliced into two sets of unit cells, shown in Figure 6; (a) is the cross-sectional unit cell, and (b) are the set of sub-unit cells that can be patterned. This pattern depends on the number of carriers used in the braiding machine. Figure 7 shows the schematic view of the top down view of the pattern of the sub-unit cells to generate a (a) 3 by 3, (b) 4 by 4, and (c) n by m braided structure. Here, letters "***C***", "***M***",

and "***E***" represents center-, middle-, and edge-unit cells, respectively. As can be seen, the weighted effects of the individual sub-unit cells are changing as the number of carriers on the braider changes.

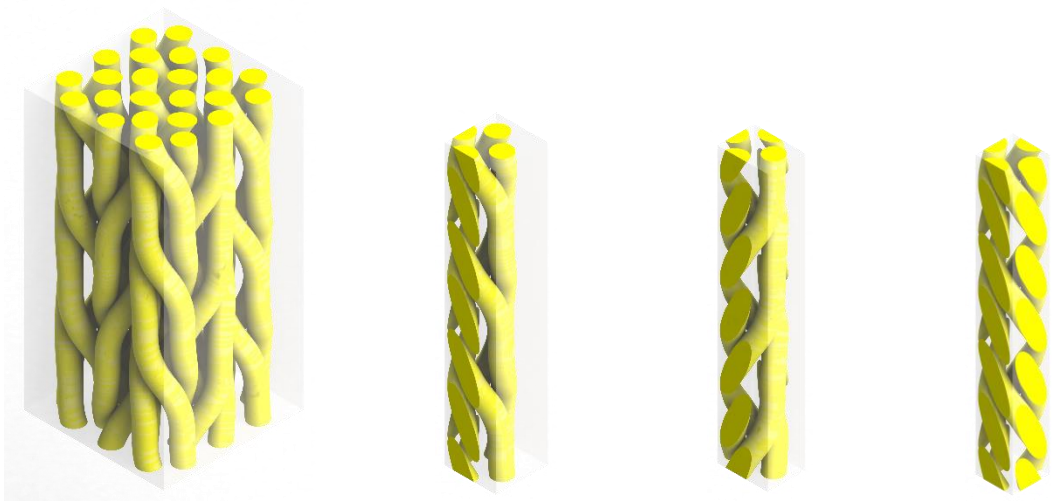

(a) (b.i) (b.ii) (b.iii)
(b)

Figure 6: 3D braiding models showing three stacked cross-sectional unit cells (a), and the three types of sub-unit cells (b), in the longitudinal direction.

C	E	C
E	M	E
C	E	C

(a)

C	E	E	C
E	M	M	E
E	M	M	E
C	E	E	C

(b)

C	E	…	E	C
E	M	…	M	E
⋮	⋮	⋱	⋮	⋮
E	M	…	M	E
C	E	…	E	C

(c)

Figure 7: Top down view of the pattern of the sub-unit cells to generate a (a) 3 by 3, (b) 4 by 4, and (c) n by m braided structure.

Utilizing commercially available FEA software (Abaqus FEA [12]), the models are imported and the material properties are set based on the macro-mechanical models presented by Kaw [13]. To apply the orthotropic, specifically transversely isotropic, material properties to the yarn, the principle directions need to be defined. To define the directions the cylindrical face of the yarn is set to be the transverse direction and the path of the yarn is set to be the axial direction (Figure 8).

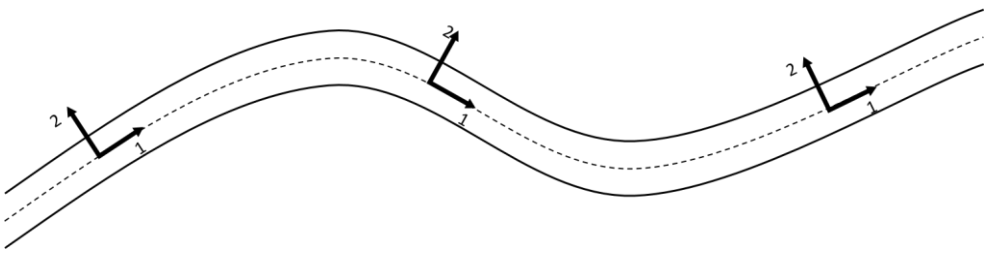

Figure 8: Discrete application of direction vectors on a yarn for transversely isotropic materials.

The interaction between the parts is created next; it is assumed that the yarns and the matrix have a perfect bond without slip. This is done by tying the cylindrical surface of the yarn together with its corresponding cavity in the matrix. Next the loading conditions and boundary conditions are applied to the FE model. A single point on the bottom surface is set to encastré (*i.e.*, all the degrees of freedom are fixed) to prevent the model from becoming unstable. The bottom surfaces are set to be free to move and rotate on the plane, but fixed in all the other degrees of freedom. The top surface is set similarly to the bottom face, with the exception that the top surface is displaced to cause a strain in the model.

For the sub-unit cells, the model is run once with the above loading/boundary conditions, and a second time with each of the cut faces constrained to their respective planes. By running the sub-unit cells twice, a range for the Young's modulus is created, that accounts for the interaction between each sub-unit cell and its neighbouring sub-unit cells. The first run, without the constraints on the cut faces, provides results for no interaction; whereby, the second run, with the cut faces constrained, provides the results for highest level of interaction between the neighbouring sub-unit cells.

2.4 Determining the Young's Modulus

The longitudinal Young's modulus is determined by the elastic definition of Young's modulus, and stress, shown in Equation (2). This is calculated by dividing the force generated in the centre of the model perpendicular to the braiding axis, by the cross-sectional area and the strain applied to the model [14].

$$E=\frac{\sigma}{\varepsilon}=\frac{F}{A\times\varepsilon} \tag{2}$$

Where, E is then Young's modulus, F is the normal force on the cross-section, ε is the strain applied, and A is the cross-sectional area as summarized in Table 1.

		Area
Cross-Sectional Unit Cell	[mm^2]	$r^2\ (16\ n\ m\ SF^2+12\ n\ SF+12\ m\ SF+9)$
Total Sub-Unit Cell (Corner)	[mm^2]	$r^2\ (16\ SF^2+12\ SF+9)$
Total Sub-Unit Cell (Edge)	[mm^2]	$r^2\ (16\ SF^2+6\ SF)$
Total Sub-Unit Cell (Centre)	[mm^2]	$r^2\ (16\ SF^2)$

Table 1: Summary of the area of the several types of unit cells, where *n* and *m* are the number of active cams in the width and depth, *r* is the yarn radius, and *SF* is the spacing factor.

3 RESULTS AND DISCUSION

3.1 Longitudinal Young's Modulus

The longitudinal Young's modulus was determined for the cross-sectional, and sub-unit cell models, with the results summarized in Table 2. The Young's modulus of the cross-sectional unit cell was found to be comparable to the fabric geometry model. However, the fabric geometry model assumes the path of the yarns is a straight line through the unit cell, it will over predict the value of the Young's modulus. The results of the cross-sectional model were confirmed, by comparing to the theoretical limits imposed by determining the properties of a unidirectional lamina at zero degrees, and at the average braid angle of the 3D braided structure.

The sub-unit cells show a variation between their different types. The difference between the results of the sub-unit cells can be accounted for by the number of surface fibers that are present in the sub-unit cell. Because the fibers on the surface of the braid are only moved every second step, the angle of these fiber decrease, increasing the Young's modulus of the sub-unit cell. As the number of cams used to create the braid increases, the number of the middle- and edge-unit cells also increases. The relationship between the number of center-, edge-, and middle- and the size of a braid is summarized in Table 3. It can be seen that as the number of active cams increases, the number of center-unit cells stays constant; where the edge-unit cells increase linearly and the middle-unit cells increase multiplicatively. Because of this multiplicative increase in the number middle-unit cells, as the braid becomes larger the properties of the braided structure will converge to the properties of the middle-unit cell.

		Young's Modulus
Cross-Sectional Unit Cell	[GPa]	10.886
Sub-Unit Cell (Corner)	[GPa]	9.215 - 11.967
Sub-Unit Cell (Edge)	[GPa]	7.789 – 10.458
Sub-Unit Cell (Middle)	[GPa]	6.472 – 9.353
Unidirectional Lamina	[GPa]	8.067 - 19.294
FGM	[GPa]	10.980

Table 2: Longitudinal Young's modulus for 3D braid composite structures.

Sub-Unit Cell Type	Number of Cells
Corner	*4*
Edge	$2\,(n + m - 4)$
Middle	$n\,m - 2\,(n + m + 2)$

Table 3: Number of each sub-unit cell for a given n by m braid, where n and m are the number of active cams in the y and z directions.

3.2 Convergence of FE Results

The results from the FEA were confirmed to have converged, by performing mesh independence analysis; as well the number of unit cells was increased to a point where the boundary condition effects were minimized. The models were all run with various mesh sizes that were decreased by an amount to roughly double the number of elements that created the model. With the use of commercial data analysis software (Statisica® [15]), it was found that the mesh had no significant effect on the modulus of the 3D braided structure. This shows that the results have converged for the models. Additionally, the models were analyzed with one, two, and three stacked unit cells to show that the FE results converged and that the effects of stresses caused by measuring the results close to the boundary conditions/loads is negligible.

4 CONCLUSIONS

Determining accurate material properties of 3D braided composites is difficult because of the complex geometry of these structures. Current models often use simplified geometry that causes inaccurate results when trying to determine the material properties. A new method and model for analyzing three-dimensional braided structures was developed. The new method was designed to take into account the undulations of the fibers in the braid structure. It was found that the models are able to produce results comparable to the previous models. Additionally, it was found that the sub-unit cells had variations between the different types (center, edge, and center). The difference in the sub-unit cells has been attributed to the inclusion of surface fibers. Future studies are required to characterize and detail the effect of these for different size braids. Additionally, experimental verifications of the models are also needed to further confirm the findings.

ACKNOWLEDGEMENTS

The authors would like to acknowledge the funds provided by Natural Sciences and Engineering Research Council of Canada (NSERC) - Discovery Grants (418533) and the University of Alberta Mechanical Engineering Department that allowed this research to be conducted.

REFERENCES

[1] L. J. Broutman and R. H. Krock, Composite Materials, vol. 3, Academic Press, Inc., 1974.

[2] Y. T. Gao, F. K. Ko and H. Hu, "Integrated Design for Manufacturing of Braided Preforms for Advanced Composites Part I: 2D Braiding," *Applied Composite Materials,* vol. 20, no. 6, pp. 1007-1023, 2013.

[3] Y. T. Gao, F. K. Ko and H. Hu, "Integrated Design for Manufacturing of Braided Preforms for Advanced Composites Part II: 3D Braiding," *Applied Composite Materials,* vol. 20, no. 6, pp. 1065-1075, 2013.

[4] F. K. Ko and T.-W. Chou, "Three-Dimensional Fabrics for Composites," *Textile Structural Composites,* vol. 3, pp. 129-171, 1989.

[5] N.Tolosana, S. Lomov and A. Miravete, "Developement of a Geometrical Model for a 3D Braiding Unit Cell Based on Braiding Machine Emulation.," in *Finite Element Modelling of Textiles and Textile Composites*, St. Petersburg, 2007.

[6] O. I. Paul, "Modelling and Simulation of Three Dimensionally Braided Composite and Mechanical Properties Analysis Using Finite Element Method (FEM)," *The International Journal of Engineering and Science,* vol. 3, no. 3, pp. 1-8, 2014.

[7] N. Tolosana, M. Carrera, R. G. d. Villoria, L. Castejon and A. Miravete, "Numerical Analysis of Three Dimensional Braided Composite by Means of Geometrical Modeling Based on Machine Emulation," *Mechanics of Advanced Materials and Structures,* vol. 19, pp. 207-215, 2012.

[8] H. Y. Yang, X. G. Zhou, J. S. Yu and Z. Luo, "Entity Simulation of Rectangle Preform for 3D Braid Composite Based on ANSYS," *Advanced Materials Research,* vol. 800, pp. 336-340, 2013.

[9] The Mathworks, Inc., "MATLAB 2017a (9.2)," mathworks.com/products/matlab.html, Natick, MA, 2017.

[10] Dassault Systèmes, "SolidWorks 2016 (Academic)," solidworks.com, Vélizy-Villacoublay, 2016.

[11] S. W. Smith, The scientist and engineerès guide to digital signal processing, San Diego, Calif.: California Technical Pub., 1997.

[12] Dassault Systèmes, "Abaqus FEA," simulia.com, Vélizy-Villacoublay, 2016.

[13] A. K. Kaw, Mechanics of Composite Materials, Boca Raton, FL: Taylor & Francis, 2006.

[14] B. v. Rietbergen, H. Weinans, R. Huiskes and A. Odgaard, "A new method to determine trabecular bone elastic properties and loading using micromechanical finite-element models," *Journal of Biomechanics*, vol. 28, no. 1, pp. 69-81, 1995.

[15] Dell, Inc., "Dell Statistica (data analysis software system), version 13," software.dell.com, 2016.